Constructing a calibration standard for photoneutron measurements by extracting cross sections of the giant-dipole resonance response in the heavy nucleus ^{169}Tm

B.S. Wellons,[1,2] R. Beyer,[3] A. Junghans,[3] L.M. Donaldson,[4] R. Neveling,[4] A. Hartmann,[3]
B. Ballester,[5,6] A. Tsinganis,[5] S. Heizitz,[7] M. Kerveno[6,8,9] and P. Adsley[1,2]
[1]*Cyclotron Institute, Texas A&M University, College Station, Texas, USA*
[2]*Department of Physics & Astronomy, Texas A&M University, College Station, Texas, USA*
[3]*Helmholtz-Zentrum Dresden-Rossendorf, Dresden, Saxony, Germany*
[4]*iThemba Laboratory for Accelerator-Based Sciences, Cape Town, South Africa*
[5]*HSCK CEN, Mol, Belgium*
[6]*University of Strasbourg, Strasbourg, France*
[7]*Joint Research Centre, Eggenstein-Leopoldshafen, Germany*
[8]*IPHC CNRS, Strasbourg, France*

Photoneutron reactions represent important tools for measuring the behavior of nuclei. Behavior such as the total dipole polarizability of nuclei, which allows understanding of symmetry energy and neutron-capture cross sections for nuclear astrophysics, nuclear reactor design, nuclear medicine and other industrial applications. Past direct measurements of photoabsorption reactions have had problems with neutron multiplicity sorting. An independent check to determine partial neutron cross sections without neutron detection is needed to confirm the simulated behavior of neutron detectors without relying on models of the nuclear reaction. The intent is that a standard calibration source for photoneu- tron measurements based on an independent experimental method will become available for future measurements. [1]

To construct a calibration standard for photoneutron reactions, high-precision (γ,1n) and (γ,2n) cross sections will be obtained. In these photoabsorption reactions a nucleus absorbs electromagnetic radiation of energies around 10-20 MeV, exciting an isovector giant dipole resonance (GDR) response in the nucleus. Macroscopically, this GDR response is characterized by the collective oscillation of nucleons within a nuclei, with de-excitation through emission of neutrons. Microscopically, GDR describes the coherent superposition of particle-hole excitations resulting from the operation on the ground state of the nucleus with a one-body operator [2]. Determining reaction cross section requires measurement of both the incident-photon fluence and the number of reaction products on an absolute scale. In this measurement the incident photon fluence is determined indirectly by normalizing to known reaction cross sections of ^{197}Au. The number of reaction products is determined by measuring the activity of radioactive residual nuclei, ^{168}Tm and ^{167}Tm.

Conducted using the γELBE facility Bremsstrahlung beamline, this measurement takes advantage of opportune half-lives of ~90 days for ^{168}Tm and ~9 days for ^{167}Tm. These half-lives ensure the presence of reaction products in the target samples well after irradiation, while still short enough that decays are often enough to be visible in a reasonable measurement window. This reaction process is visualized in Figure 1, where the characteristic γ rays from erbium (^{168}Er and ^{167}Er) are the measurement signatures.

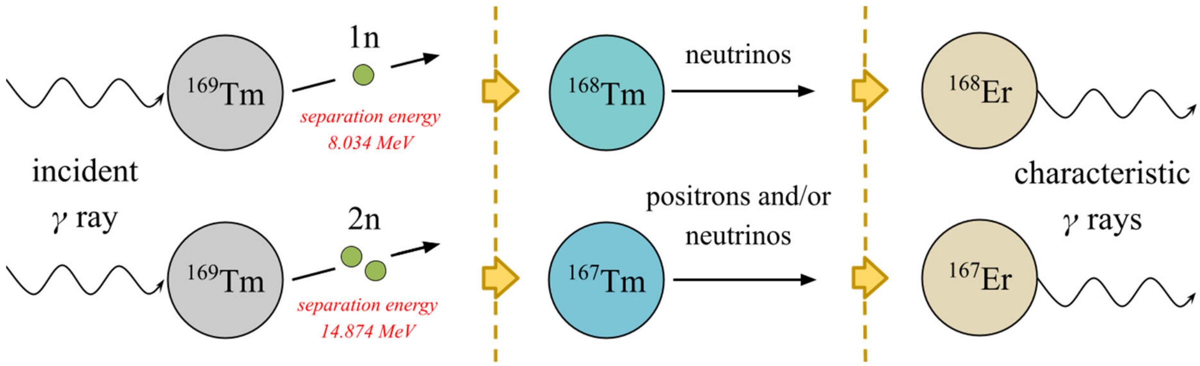

Fig. 1. Diagram of the photoneutron reactions 169Tm(γ, 1n) and 169Tm(γ, 2n), showing their resulting isotopes decaying with characteristic γ rays, and including the neutron separation energies for one neutron versus two.

These γ rays from erbium transitions to the ground state represent the final energy signatures from the photoactivation pathway, as both erbium products are stable isotopes. Since both thulium reaction products have above a 99% chance of decaying through the displayed channels, only clear energy signatures from these decays are expected, baring any of the sample's self absorption/capture of reaction ejecta.

The target stack in order of incident beam was 169Tm, 197Au, 99Mo, 197Au, and 58Co, the later three being from collaborators. Irradiations were done at electron-beam endpoint energies 8.5 MeV to 18.5 MeV at 0.5-MeV steps (19 total). An HPGe detector from γELBE was used in data collection; its high energy resolution key in differentiating γ lines in recorded spectra.

In photoactivation experiments, the number of radioactive nuclei $N_{act}(E_0)$ produced is propor- tional to the target atoms N_{tar} times the integral of the absolute photon fluence $\Phi_\gamma(E, E_0)$ times the photodisintegration cross section $\sigma_{\gamma,n}(E, E_0)$ integrated from the reaction threshold energy E_{th} up to the endpoint energy E_0 of the Bremsstrahlung spectrum [3]:

$$\mathrm{N_{act}(E_0)} = \mathrm{N_{tar}} \cdot \int_{E_{th}}^{E_0} \sigma_{\gamma,n}(\mathrm{E}, \mathrm{E_0}) \cdot \Phi_\gamma(\mathrm{E}, \mathrm{E_0})\, d\mathrm{E}. \tag{1}$$

The target atoms is a known parameter in the experiment, so the photon fluence and number of activations need to be extracted experimentally. The number of radioactive nuclei is determined experimentally by measuring the activity of the irradiated sample using [3]:

$$\mathrm{N_{act}(E_0)} = \frac{\mathrm{N}_\gamma(\mathrm{E}_\gamma, \mathrm{E_0}) \cdot \kappa_{corr}}{\varepsilon(\mathrm{E}_\gamma) \cdot p(\mathrm{E}_\gamma)} \tag{2}$$

where $N_\gamma(E_\gamma, E_0)$ is the dead-time and pile-up corrected full-energy peak counts of the observed transition E_γ, $\varepsilon(E_\gamma)$ is the absolute efficiency of the detector at energy E_γ, and $p(E_\gamma)$ is the emission probability of the transition photon of energy E_γ. The detector efficiency is determined through calibration data collected from γELBE-facility sources ^{137}Cs, ^{60}Co, and ^{152}Eu. The emission probabilities corresponding to the relevant states in ^{168}Er and ^{167}Er are taken from the National Nuclear Data Center (NNDC) found in Refs. [4, 5]. The κ_{corr} factor connects to the number of radioactive nuclei given the number of decays we observe during our measurement time (t_{meas}). It accounts for the activated atoms which decayed during the irradiation time (t_{irr}) and between the end of irradiation and beginning of measurement (t_{loss}). The equation for κ_{corr} is given by

$$\kappa_{corr} = \frac{e^{\lambda \cdot t_{loss}}}{1-e^{-\lambda \cdot t_{meas}}} \cdot \frac{\lambda \cdot t_{irr}}{1-e^{-\lambda \cdot t_{irr}}} , \tag{3}$$

where $\lambda = \ln(2)/tt$, with half lives ($t_{1/2}$) from NNDC in Refs. [4, 5]. The activation yield at a given endpoint energy, $Y_{act}(E_0)$, is a useful equation for visualizing the results and is given by

$$Y_{act}(E_0) \frac{N_{act}(E_0)}{N_{tar}} \tag{4}$$

The Bremsstrahlung nature of photon creation results in energies which vary as in the on-site measured distribution displayed in Fig. 2. Photon fluence curves are determined for each endpoint energy.

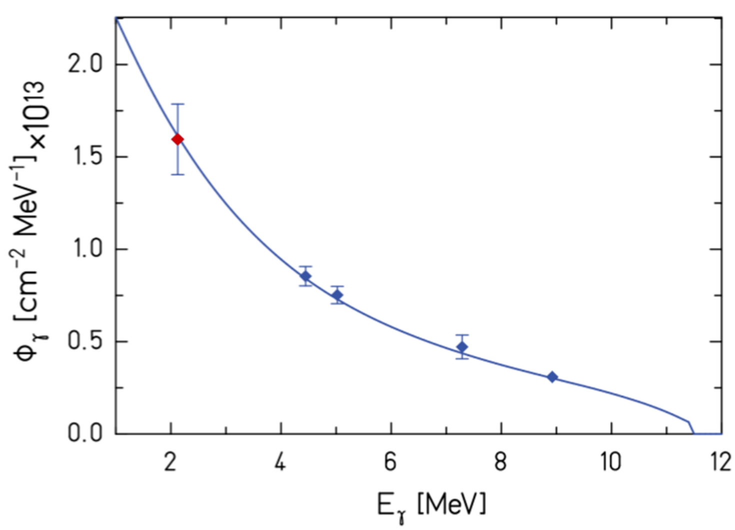

Fig. 2. Absolute photon fluence measured previously at γELBE and compared with the Seltzer and Berger [6] Bremsstrahlung spectra including hardener corrections. Reprinted from Ref. [3].

To extract the photoneutron cross sections, the "photon-difference" method from Ref. [7] is used. This method involves taking the difference in activation yields from one endpoint energy and the previous endpoint-energy step. This subtraction gives the cross section from a sliver of photon energies, whose thickness equals the endpoint-energy step width.

Initial observations of measured spectra indicate both ^{169}Tm(γ, 1n) and ^{169}Tm(γ, 2n) pathways have statistically significant experimental signatures above the (γ, 2n) separation energy (S_{2n}) of 14.874 MeV.

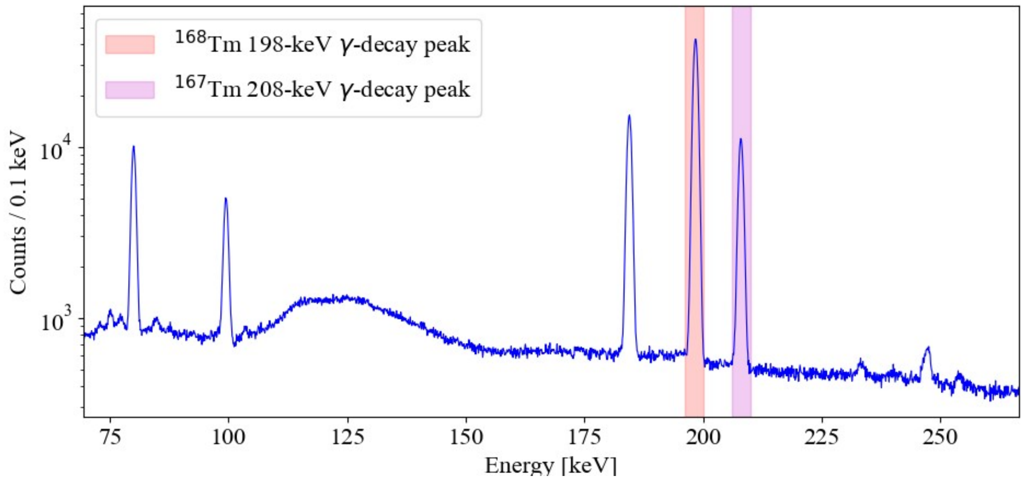

Fig. 3. Recorded spectra of target Tm 27, irradiated with 18-MeV endpoint energy γ-rays. Including prominent 198-keV and 208-keV decay channel peaks from 168Tm populated by 169Tm(γ,1n), and 167Tm, populated by 169Tm(γ,2n), respectively.

Fig. 3 displays one such spectra, with prominent decay peaks highlighted. This implies that both (γ, 1n) and (γ, 2n) reaction cross sections can be extracted

Cross sections are yet to be extracted, but a comparison of the ^{169}Tm(γ, 1n) experimental yields was made to those predicted using current EXFOR photoneutron cross section data in Ref. [8]. The experimental-activation yields for ^{169}Tm(γ, 1n) were obtained using Eq. 2 and Eq. 4. The peak counts were initially taken from only the most prominent decay channel, 198 keV, as seen top left in Figure 4. The predicted yields were calculated using Eq. 1 into 4, with the photoneutron cross sections taken from EXFOR, Ref. [4], and the absolute photon fluence estimated using our gold activation results.

The fluence estimation was done as follows. Calculating Eq. 2, with only the most prominent decay channel of 356 keV, gives our ^{197}Au(γ, 1n) experimental activations. This value can be substituted, along with ^{197}Au(γ, 1n) EXFOR photoneutron cross sections taken from Ref. [9, 10], into Eq. 1. This allows us to

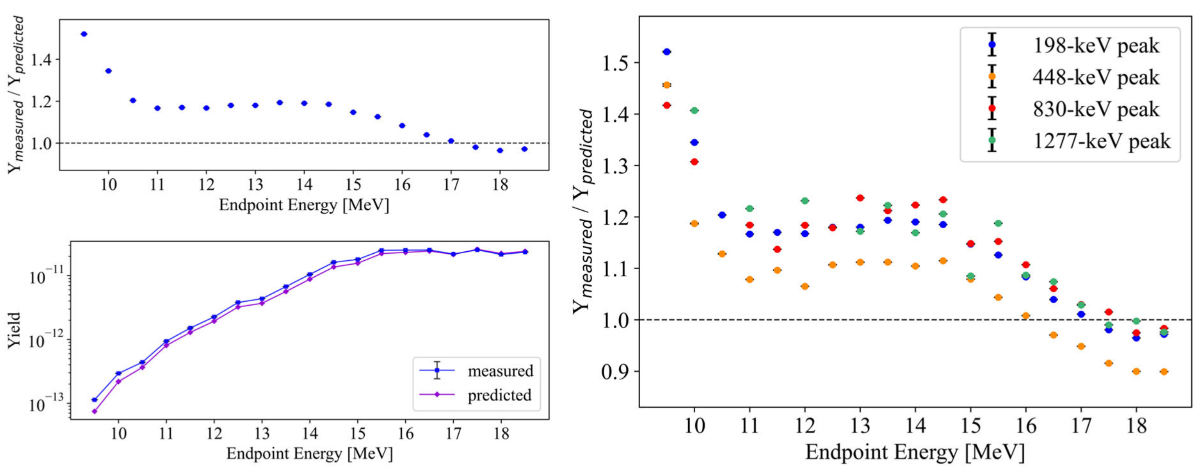

Fig. 4. (Top Left) Ratio of the measured over predicted activation yields from the (γ, 1n) reaction using the 198-keV peak, at every endpoint energy E0. (Bottom Left) The measured and predicted activation yield curves displayed separately versus endpoint energy. (Right) Ratios of the measured over predicted activation yields from the (γ, 1n) reaction using various prominent peaks.

estimate an absolute photon fluence, whose predefined shape is created using a differential Bremsstrahlung creation formula. The solution is a scaling factor we can use to the estimated fluence shape, which when incorporated replicates the experimental photon fluence at each irradiations endpoint energy.

The yield comparison made with the 198-keV peak, top left of Figure 4, displays a measured yield consistent with roughly 20% above the predicted. Bottom left in Figure 4 we can see the individual yields for comparison. The sharp spike at the lowest energies might be explained by an overestimation of low energy photon creation, or simply from deviations in values of small relative magnitudes being over represented when taken as a ratio. a drop in the measured (γ, 1n) yield ratio is also observed just above the S_{2n} threshold.

To explore the 20% scaling anomaly experimental activation yields were again measured, using peaks at varied energies. This result is shown in the right side of Figure 4. One observation is the 448-keV peak, which happens to be closest in energy to gold's 356-keV peak used in the fluence calculation, only deviates by about 10%. This may be due to errors in the energy dependence of the absolute detector efficiency, since we are currently using previous efficiency measurements. If our absolute detector efficiencies are offset, as the thulium peak energies approach gold's so will the values of efficiency, effectively removing the affect of this offset.

More analysis must be conducted to fully understand this affect, beginning with the calculation of our own detector efficiencies. Inclusion of the (γ, 2n) yields might be worthwhile, to see its effect on the apparent dipping above the S_{2n} threshold.

[1] V. Varlamov, B. Ishkhanov, V. Orlin, Phys. Rev. C **96**, 044606 (2017). doi:https://doi.org/10.1103/PhysRevC.96.044606.

[2] M. Harakeh, A. van der Woude, *Giant Resonances: Fundamental High-Frequency Modes of Nuclear Excitation*, Oxford University Press Inc., New York, 2006.

[3] C. Nair, M. Erhard, A.R. Junghans, D. Bemmerer, R. Beyer, E. Grosse, J. Klug, K. Kosev, G. Rusev, K.D. Schilling, R. Schwengner, and A. Wagner, Phys. Rev. C **78**, 558 (2008). doi:http://dx.doi.org/10.1103/PhysRevC.78.0558.

[4] C. M. Baglin, Nuclear data sheets for A = 168, Nuclear Data Sheets **111 (7)**, 1807 (2010); doi:https://doi.org/10.1016/j.nds.2010.07.001;https://www.sciencedirect.com/science/article/pii/S0090375210000682

[5] B. Singh, J. Chen, Nuclear structure and decay data for A=167 isobars, Nuclear Data Sheets **191**, 1 (2023); doi:https://doi.org/10.1016/j.nds.2023.08.001.
URL https://www.sciencedirect.com/science/article/pii/S0090375223000522

[6] S.M. Seltzer, M.J. Berger, Bremsstrahlung energy spectra from electrons with kinetic energy 1 kev–10 gev incident on screened nuclei and orbital electrons of neutral atoms with z = 1–100, Atomic Data and Nuclear Data Tables **35**, 345 (1986). doi:https://doi.org/10.1016/0092- 640X(86)90014-8.

[7] O. V. Bogdankevich, F.A. Nikolaev, Methods in Bremsstrahlung Research, Academic Press, New York and London, 1966.

[8] T. Kawano, Y. Cho, P. Dimitriou, D. Filipescu, N. Iwamoto, V. Plujko, X. Tao, H. Utsunomiya, V. Varlamov, R. Xu, R. Capote, I. Gheorghe, O. Gorbachenko, Y. Jin, T. Renstrøm, M. Sin, K. Stopani, Y.

Tian, G. Tveten, J. Wang, and M. Wiedeking, IAEA photonuclear data library 2019, Nuclear Data Sheets **163**, 109 (2020); doi:https://doi.org/10.1016/j.nds.2019.12.002.

[9] O. Itoh, H. Utsunomiya, H. Akimune, T. Kondo, M. Kamata, T. Yamagata, H. Toyokawa, H. Harada, F. KitataniI, S. Goko, C. Nair, and Y.-W. Lui, Journal of Nuclear Science and Technology **48** (5) 834 (2011);doi:10.1080/18811248.2011.9711766.
URL https://www.tandfonline.com/doi/abs/10.1080/18811248.2011.9711766

[10] C. Plaisir, F. Hannachi, M. Tarisien, M. Alenard, V. Meot, G. Gosselin, P. Morel, B. Morillon, Eur.Phys. J. A **48**, 68(2012); doi:10.1140/epja/i2012-12068-7.
URL https://link.springer.com/article/10.1140/epja/i2012-12068-7#citeas